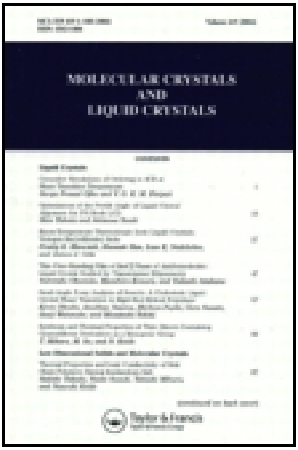

Molecular Crystals and Liquid Crystals

Publication details, including instructions for authors and subscription information:
http://www.tandfonline.com/loi/gmcl20

Thermal Behavior of a Cationic Mesogen Intercalated into Clay Interlayer

N. Iyi [a] , Y. Kaneko [a] , T. Fujita [a] , S. Nagamani [b] & C. Yelamaggad [b]

[a] Advanced Materials Laboratory, National Institute for Materials Science (NIMS), Namiki 1-1, Ibaraki, Tsukuba, 305-0044, Japan

[b] Centre for Liquid Crystal Research, P. B. No. 1329, Jalahali, Bangalore, 560 013, India

To cite this article: N. Iyi, Y. Kaneko, T. Fujita, S. Nagamani & C. Yelamaggad (2004): Thermal Behavior of a Cationic Mesogen Intercalated into Clay Interlayer, Molecular Crystals and Liquid Crystals, 414:1, 49-61

To link to this article: http://dx.doi.org/10.1080/15421400490427494

Mol. Cryst. Liq. Cryst., Vol. 414, pp. 49–61, 2004
Copyright © Taylor & Francis Inc.
ISSN: 1542-1406 print/1563-5287 online
DOI: 10.1080/15421400490427494

THERMAL BEHAVIOR OF A CATIONIC MESOGEN INTERCALATED INTO CLAY INTERLAYER

N. Iyi, Y. Kaneko, and T. Fujita
Advanced Materials Laboratory, National Institute for Materials Science (NIMS), Namiki 1-1, Tsukuba, Ibaraki 305-0044, Japan

S. Anitha Nagamani and C. V. Yelamaggad
Centre for Liquid Crystal Research, P. B. No. 1329, Jalahali, Bangalore 560 013, India

*To investigate the thermal behavior of a mesogen in confined geometry, a cationic mesogen (***Az***; $NO_2{-}C_6H_4{-}N{=}N{-}C_6H_4{-}O{-}(CH_2)_6{-}N^+C_2H_5(C_2H_4OH)_2$) was incorporated into the interlayers of four clay mineral and synthetic swelling mica hosts. Incorporation caused increase in the basal spacings of which two types were observed, a larger (ca. 3.4 nm) and a smaller one (ca. 2.1–2.4 nm). Interdigitated antiparallel arrangement of the guest with its long axis perpendicular to the layer was assumed for the larger basal spacing, and inclined arrangement was for assumed the smaller one. Smectic behavior was exhibited only for the guest molecules in the interdigitated antiparallel arrangement.*

Keywords: intercalation; liquid crystal; organo-clay complex; smectic

INTRODUCTION

Intercalation is a process that involves the reversible incorporation of guest molecules into layered host materials while maintaining the structural features of the host [1]. The attractive feature of intercalation process is the expandability of the interlayer spacing of layered host materials. To date, a variety of host–guest systems have been reported with unique structures and properties [2]. The microscopic structure of the guest–host system can be designed by the appropriate selection of the guest and the host and, sometimes, new properties appeared by interaction between the guest and host [3]. Various layered materials such as graphite, clay

Address correspondence to N. Iyi, e-mail: iyi.nobuo@nims.go.jp

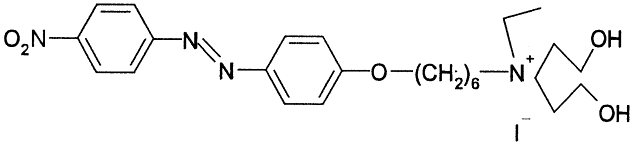

FIGURE 1 Molecular structure of mesogenic quaternary ammonium ion (**AzI**) employed as guest molecules for the intercalation.

minerals, transition metal dichalcogenides, etc. have been used as hosts. Among these, clay minerals have been extensively used for obtaining functional materials because composites can be prepared by simple ion exchange procedure [4,5]. The guest molecules are either surfactants or polar aromatic compounds, and many surfactant–clay composites have been prepared and used as additives for polymer and adsorbents for organic pollutants [6–9]. Some of the organo-clay composites comprising of dialkyldiammonium ion have been reported to show gel in the liquid crystal phase transition.

The interaction between liquid crystals (mesogens) and clay minerals have also been reported to some extent [10–31]. Clay minerals have been used as additives to change or improve the thermal behavior of liquid crystals. Recently, a novel memory effect was observed by addition of clay mineral intercalated with a variety of organic cations to liquid crystals [12,13]. This result suggested the possibility that interaction between liquid crystals and clay would lead to new properties if the clay is appropriately modified. Though there have been only few reports in which composite systems are formed by intercalating liquid crystals in the layers of clay minerals, such composites appear to be promising materials from both basic research and practical application viewpoints.

In the present study, we have incorporated a cationic moiety of a smectic liquid crystal **AzI** (NO_2-C_6H_4-N=N-C_6H_4-O-$(CH_2)_6$-$N^+C_2H_5(C_2H_4OH)_2I^-$) (Figure 1) as a guest in the confined interlayer spacing of synthetic swelling mica and some clay minerals by cation exchange reactions. In this report, we make an effort to study the effect of the guest on the host (changes in basal spacing) and the effect of the host on the guest (changes in mesomorphic behavior).

RESULTS AND DISCUSSION

The molecular structure of **AzI** is shown in Figure 1 and was synthesized following the literature procedure [14]. The mesomorphic behavior of **AzI** was evaluated with the help of polarizing microscopic, calorimetric, and X-ray studies. The phase sequence and temperatures (K 53°C

Sm 178°C I) were found to be consistent with the reported temperatures. Figure 2 shows DSC thermograms of heating and cooling cycles. For the X-ray investigations, droplets of aqueous **AzI** solution were applied on a clean and untreated glass plate and, after evaporation of water, X-ray profile was measured from $2\theta = 1.5^\circ$ to 20° by using powder X-ray diffractometer. In the X-ray profile, at room temperature ($00l$) diffractions were observed up to $l = 5$ without other *hkl* diffractions and with the basal spacing being 2.78 nm. Figures 3(a) and 3(b) show the change in X-ray powder diffraction profiles with respect to change in temperatures. By heating, the basal spacing decreased a little to 2.66 nm, and at a temperature of 74°C new peaks appeared with basal spacing 3.13 nm. This new peak prevailed up to 92°C. Within the intermediate temperature range, i.e., 74–92°C, there was another series of ($00l$) diffractions with observed interlayer space of 1.90 nm, suggesting layered structure. These reflections appeared only in this temperature range, so it indicates an ordered mixed-layer structure. These results are consistent with the previous report [14].

Ujiie and Iimura [14] estimated the molecular length of the quaternary ammonium ion as 2.45 nm. We have calculated the molecular dimensions using a semiempirical molecular dynamics program (MM2 in Chem3D, Cambridge Soft), taking the van der Waals radius into consideration. The molecular length including I^- ion was 2.60 nm, and the length without I^- (**Az**) was about 2.45 nm. Since the interlayer space was 3.1 nm, **AzI** was assumed to have interdigitated arrangement with aromatic rings overlapped. This result is consistent with Ujiie and Iimura's model [14].

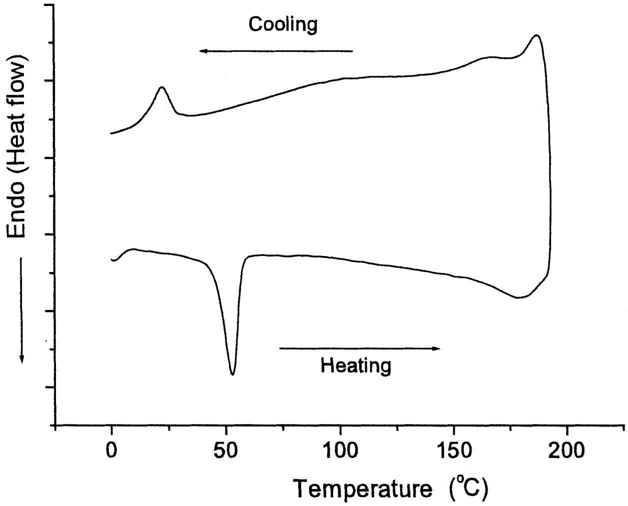

FIGURE 2 DSC thermograms of the heating and subsequent cooling cycles of **AzI**.

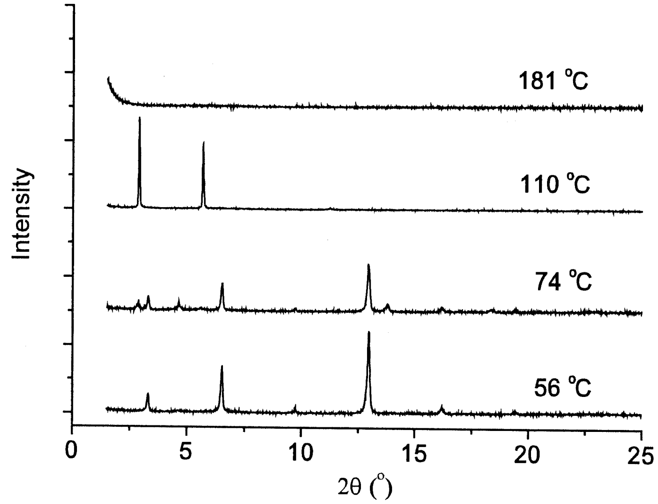

FIGURE 3 (a) X-ray powder diffraction profiles obtained at different temperatures for **AzI**. (b) Change in basal spacing of **AzI** with change in temperature.

Synthetic swelling mica, Li taeniolite (**TN**, $LiMg_2LiSi_4O_{10}F_2$), and commercially available clay materials such as Kunipia montmorillonite (**Kp**, $Na_{0.33}[Al_{1.66}Mg_{0.33}]Si_4O_{10}(OH)_2$), Smecton SA (**Sm**, $Na_{0.33}Mg_3[Si_{3.66}Al_{0.33}]$-$O_{10}(OH)_2$), and Lithium hectorite (**HT**, $Li_{0.33}[Mg_{2.66}Li_{0.33}]Si_4O_{10}F_2$) have been used as host inorganic materials for the preparation of complexes. Host–guest complexes were prepared by dispersing host and guest materi-

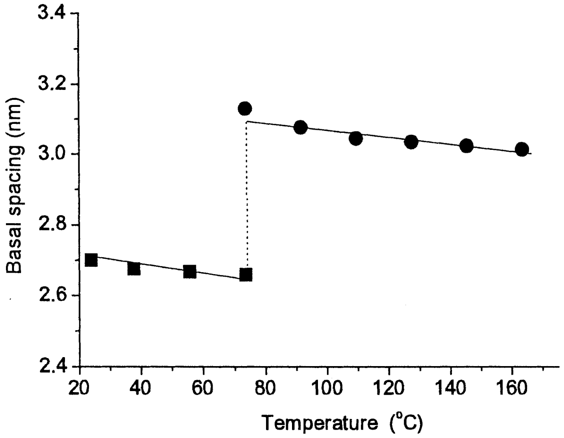

FIGURE 3b Continued.

als together in a water-ethanol (1:1) mixture under ultrasonification. In this reaction, **Az** (cationic moiety of **AzI**) is incorporated into interlayer space. In this article, the products are abbreviated as **Az/TN**, **Az/Kp**, **Az/Sm**, and **Az/HT**. For the comparison, X-ray profile of TN is shown (Figure 4, top portion). **TN** has the basal spacing of 1.52 nm at high humidity RH $> 60\%$ and 1.23 nm at low humidity (RH $< 60\%$)(RH = relative humidity). The layer thickness is estimated to be about 0.92 nm, and Li^+ and water molecules (nearly 0.3 nm) form bi- and tri-layers, leading to the basal spacing mentioned above.

The complex **Az/TN** showed a basal spacing of $d_{00l} = 3.45$ nm (Figure 4, bottom). The basal spacings of the complexes with other clay minerals were 3.5 nm (broad peak) for **Az/HT**, 2.28 nm for **Az/Kp**, and 2.1 nm (broad) for **Az/Sm** (Table 1). As a secondary phase, 3.5 nm phase was also observed for **Az/Kp** and 2.4 nm phase for **Az/HT**. Increase in basal spacings of the resulting complexes indicated the **Az** was successfully incorporated into the interlayer space of clay minerals. As the molecular length of **Az** is 2.45 nm, interdigitated arrangement (homeotropic orientation) of **Az** molecules would lead to a total basal spacing of about 3.4 nm. Basal spacings of the complexes **Az/TN** and **Az/HT** were comparable with this value, so in these complexes, **Az** molecules take interdigitated structure with its long axis almost perpendicularly oriented to the silicate layer (Figure. 5). On the other hand, for **Az/Sm** and **Az/Kp**, we assumed the incorporated **Az** molecules are rather inclined at an angle about 30°.

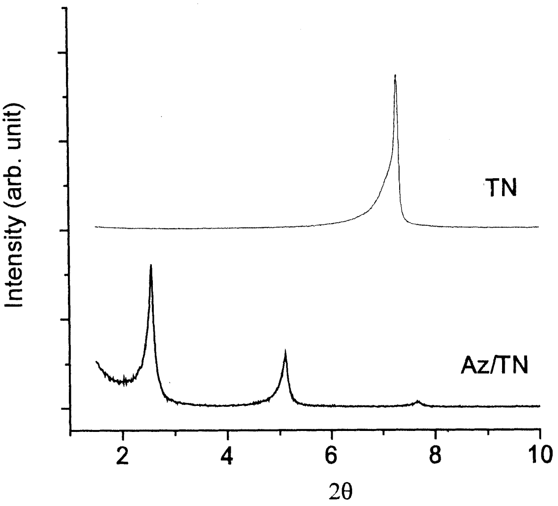

FIGURE 4 X-ray profiles of host synthetic mica **TN** (top portion) and complex **Az/TN**.

TABLE 1 Composition and Basal Spacings of the Obtained Az/clay Complexes

	Elemental analysis results (wt%)				
Specimen	C	H	N	Az/clay mole ratio	Basal spacing (nm)
Az/TN	28.8	3.4	5.9	0.69	3.45
Az/Kp	24.7	3.1	5.1	0.52	2.28(+3.5)
Az/Sm	21.4	2.9	4.4	0.45	2.10
Az/HT	20.6	2.3	4.2	0.40	3.50(+2.4)

The UV-VIS spectra were taken for **AzI** solutions and **Az/clay** complexes. For aqueous solution of AzI (0.1 mM), and a broad single peak was observed at 372 nm (Figure 6). Because more diluted aqueous solution of **AzI** (0.001 mM) exhibited the same spectrum, this absorption was assigned to monomer state. Even by using ethanol for the solvent, change in absorption profile was not observed. The ethanolic **AzI** solution was applied on a quartz plate and, after dried up, the spectrum of **AzI** film was measured in transmittance mode. Layer stacking of **AzI** was reconstructed even after this operation. **AzI** film, which was assumed to take interdigitated arrangement with **Az** molecules oriented perpendicular to the layer, showed very large blue-shift of the peak to 349 nm. The relationship between spectral characteristics and molecular orientation of azobenzene chromophore has already been reported [17], and large blue-shift of π–π^* transition band was reported for the interdigitated antiparallel arrangement of azobenzenes as shown in Figure 5. This large blue shift

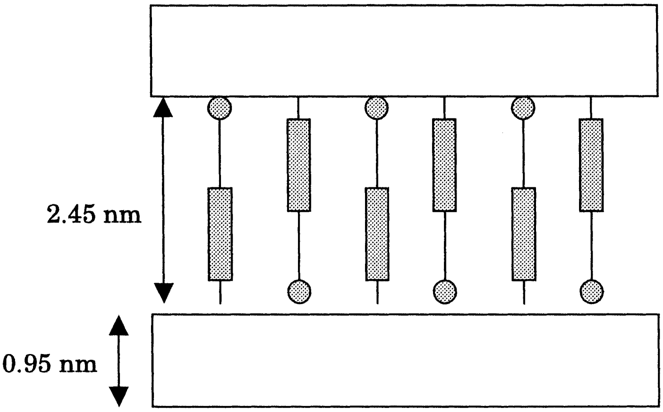

FIGURE 5 Schematic representation of the arrangement of **Az** species in the interlayer space of **Az/TN** complex—the antiparallel interdigitated arrangement with molecular axis perpendicular to the silicate layer.

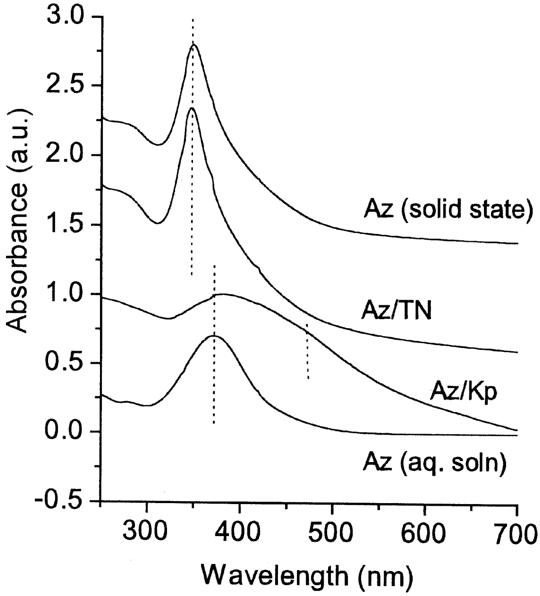

FIGURE 6 UV-VIS spectra of **AzI** in aqueous solution and **AzI** film (soild state). Absorption spectra of **Az/TN** and **Az/Kp** complexes are also shown.

can be assigned to lateral arrangement of azobenzene moiety, which supports the interdigitated arrangements of **Az** with its molecular axis nearly perpendicular to the layer assumed by the interlayer distance. UV-VIS measurement was also conducted for **Az/Clay** complexes (Figure 6). The peak position of the absorption band for **Az/TN** is at about 347 nm, and almost the same as that for the solid-state **AzI** film. **Az** molecules in the **Az/TN** complex probably take the same interdigitated arrangement. The complex, **Az/HT** showed similar features, but with shoulder absorbance, which indicates some amount of monomer state. The broad peak of **Az/Kp** and **Az/Sm**, centered at about λmax = 381 nm and with broad shoulder extending to 470 nm, implies the **Az** molecules are present in the monomer state mixed with other **Az** species. Broad shoulder at longer wavelength for these complexes would be caused by the head-and-tail arrangement of **Az** because such arrangement is reported to cause red-shift of the absorption peak. This is consistent with the molecular arrangements of **Az** inclined at about 30° to the silicate layer as assumed from XRD data. Thus, UV-VIS spectrum data are in well consistent with the X-ray results.

The microanalytical data of the complexes **Az/TN, Az/Kp, Az/Sm** and **Az/HT** have been listed in Table 1. On the basis of C-content, the mole ratio of Az/clay can be calculated. Here, the amount of incorporated **Az** was calculated per unit formula of the host. It is well known that clays with higher charge density can incorporate more cations in the interlayer space, which would increase the angle between the cations and the silicate layers, and thus leading to an increase in the basal spacing. As expected, **Az/TN** complex, having the highest **Az/clay** mole ratio, has the largest basal spacing, and **Az/Sm** complex, having the lowest **Az/clay** mole ratio, showed the smallest basal spacing. But the exceptional behavior observed for **Az/HT** could be due to the high crystallinity and/or the inhomogeneous charge density distribution of the silicate layer.

DSC scans of **Az/TN** (Figure 7(a))and **Az/HT** showed an endothermic transition at 70–95°C (on heating) similar to **AzI** itself. The starting host materials were also examined under the same DSC conditions, but they did not show any apparent transition. Only gradual baseline change occurred above 100°C, which is probably due to the evaporation of water. The endothermic transition temperature decreased upon repeated heating–cooling cycles. At first heating, endothermic transition temperature was observed at 95°C, but in the third heating it dropped to 85°C for **Az/TN**. A similar behavior was also seen in **AzI**. In **AzI**, the endothermic transition takes place at 77°C, but on the third heating it dropped to 55°C. Even after heating the **Az/TN** sample to 200°C, there was no peak corresponding to the phase transition to the isotropic phase. This system seems to be extremely sensitive to heat and undergoes thermal decomposition at

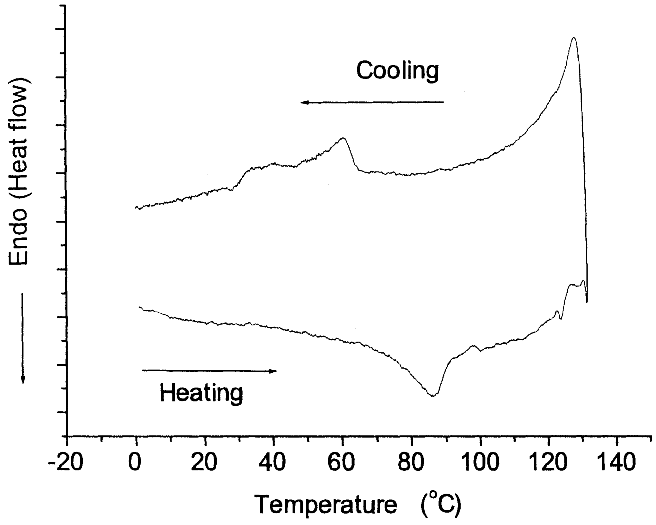

FIGURE 7 DSC thermograms of first heating and subsequent cooling cycles of (a) **Az/TN** complex and (b) **Az/HT** complex.

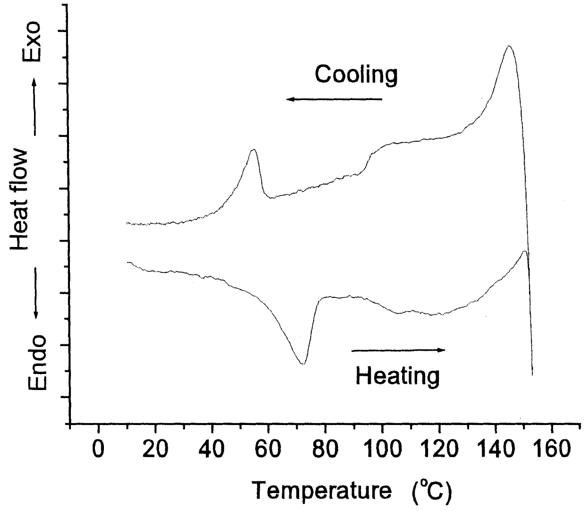

FIGURE 7b Continued.

higher temperatures. Similar DSC profile was obtained for **Az/HT** (Figure 7(b)). It implies that the **Az/clay** complexes, which have interdigitated structure with **Az** oriented perpendicularly to the silicate layer, showed similar DSC profile to the smectic **AzI**. On the other hand, no apparent thermal event was observed for **Az/Kp** and **Az/Sm**. It could be due to the highly tilted arrangement of the incorporated **Az** molecules for these complexes. The transition temperature is higher in Az/clay system than that for AzI itself. Generally speaking, the thermal stability of organics is enhanced when they are incorporated in the interlayer space of the clay minerals. This is because the organic moieties are protected by the rigid inorganic layers.

Attempts to observe the change in basal spacing of **Az/TN** complex, with temperature were made. There was a slight decrease in the basal spacing as the temperature is increased to 60°C, which could be attributed to the evaporation of adsorbed water in the interlayer space; similar change was observed for the **TN** incorporating long chain alkyl (octadecyl) ammonium ion (**C18/TN**). Then an abrupt change in basal spacing from 3.38 nm to 3.53 nm was observed at 60–80°C (Figure 8). As already described in the previous section, **AzI** ion complex also exhibited an abrupt increase in the d_{00l} from 2.7 nm to 3.1 nm. With respect to the change in basal spacing and transition temperature, **Az/TN** and **AzI** show the same trend.

As already pointed out in the introduction section, gel-to-liquid-crystal transition has been observed for the clay intercalated with dialkyldiammonium ion [6–9]. Such phase transition was assumed by the change in the

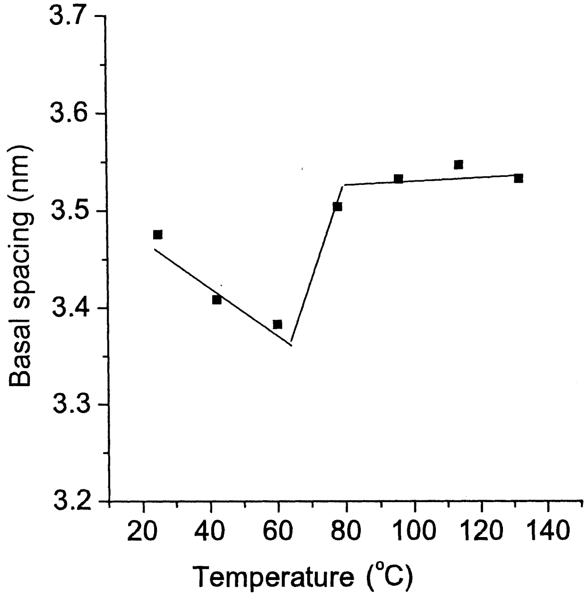

FIGURE 8 Change in the basal spacing of **Az/TN** with the change in temperature.

properties of probe molecules, reflecting the change in the environment, i.e., the state of alkyl layer. Vaia et al. [18] assumed partially ordered alkyl chain aggregation in the interlayer space. However, the detailed nature of the liquid crystal-like phase was not revealed so far. In the present study, we used an azo derivative (AzI), which exhibited the smectic liquid crystal (smectic A) phase for itself. For this reason, we could compare the DSC profiles for AzI and Az/clay complexes. By using X-ray diffraction (XRD) and UV-visible light adsorption spectra (UV-VIS), we assumed some of the Az/clay composites exhibited the antiparallel interdigitated structure with the organic molecular nearly perpendicular to the silicate layer. This arrangement is similar to that of smectic A. Considering that the similar thermal event to AzI having smectic A structure also occurred in the Az/clay composites with interdigitated Az arrangement, it is highly possible that a thermotropic smectic A phase is formed.

SUMMARY

In conclusion, we have successfully incorporated a mesogenic quaternary ammonium ion into the interlayer spacing of synthetic micas and clay minerals. The investigations on the change in the basal spacings of the complexes suggest that the ionic mesogens attain either interdigitated structure in which **Az** molecules are arranged almost perpendicularly to the layer or titled structure in which the molecules inclined at an angle with respect to the layers. DSC, XRD, and UV-VIS data revealed that, only sin the case of interdigitated structure, the guest molecule retains the mesomorphic behavior within the layers.

EXPERIMENTAL

General Information

The required chemicals, namely 4-nitroaniline, diethanolamine, and 1,6-dibromohexane were obtained from Lancaster Company. These chemicals were used as received, while the solvents obtained from local sources were dried following standard procedures. A synthetic swelling mica, lithium taeniolite (**TN**, $LiMg_2LiSi_4O_{10}F_2$), was obtained from Topy Industries Co. LTD. Other clay materials, Kunipia montmorillonite (**Kp,** $Na_{0.33}[Al_{1.66}Mg_{0.33}]Si_4O_{10}(OH)_2$) and Smecton SA (**Sm**, $Na_{0.33}Mg_3[Si_{3.66}Al_{0.33}]O_{10}(OH)_2$), were obtained from Kunimine Industries Co. LTD, and Lithium hectorite (**HT**, $Li_{0.33}[Mg_{2.66}Li_{0.33}]Si_4O_4F_2$) was received from Topy Industries Co. LTD. The cation exchange capacity (CEC; in meq/100 g) was 102 for **TN**, 101 for **Kp**, 73 for **Sm**, and 45 for **HT**. Thin layer chromatography (TLC) was performed on aluminium sheets precoated with silica gel (Merck, Kieselge10, and F254). Column chromatographic separations were performed using silical gel (60–120 mesh). ^1H NMR spectra were recorded using a Bruker AMX-400 (400-MHz) spectrometer and the chemicals shifts are reported in parts per million (ppm) relative to tetramethylsilane (TMS) as an internal standard. CHN analysis was conducted using Perkin-Elmer 2400 II CHN element analyzer with acetanilide as the standard material for characterizing the composition of the starting guest **AzI** and the yielded **Az/clay** complexes.

The phase transition was measured for specimens sealed in aluminum vessels by using a differential scanning calorimeter DSC3200S with a cooling unit CU9400 (MAC Science, Co., LTD) at 10°C/min heating-cooling rate between $-10°C$ and 100°C. The phase was confirmed with a Nikon polarizing microscope equipped with a Mettler FP900 hot stage system. XRD of the complex was conducted between $2\theta = 1.5$ to 20° at a scanning speed of $2\theta = 2^\circ$/min using a RINTI1200 (RIGAKU) diffractometer with Ni-filtered CuKα radiation ($\lambda = 0.15418\,nm$). A temperature-controlled hot plate was placed under a glass plate holder of the specimen mounted on the goniometer. The temperature at the specimen was calibrated by direct temperature measurement under the same experimental conditions. UV-VIS of complexes were recorded at 900–250 nm by a V-550DS (JASCO Co. Ltd.) in transmittance mode at 400 nm/min scanning.

Preparation of Bis(2-hydroxyethyl)ethyl (6-(4-(4-nitrophenyl)azo)phenyl)oxyhexyl AmmoniumIodide (AzI)

The quaternary ammonium iodide of azobenzene derivative (**AzI**) was synthesized following a procedure described by Ujiie and Iimura [14]. ^{1}H NMR (400 MHz, $CDCl_3$): δ 8.5–8.2 (d, 2H), 8.2–7.8 (d, 4H), 7.2–6.9 (d, 2H), 5.5–5.0 (bs, 2H), 4.5–3.8 (m, 6H), 3.8–3.2 (m, 6H), 2.4–1.4 (m, 8H).

Preparation of Complexes

Twenty five milligrams of the host material was dispersed in 5 ml of water by ultrasonification. To this aqueous suspension, **AzI** (30 mg, 0.051 mM) was added in 10 ml of water–ethanol mixture (1:1). The mixture was agitated at 50°C for 2 days. The resulting suspension was filtrated by millipore filter (0.2 μm) and was washed with water followed by ethanol, and then dried at room temperature under vacuum. For UV-VIS measurement, ion exchange was conducted for thin clay films formed on quartz plates. A few drops of aqueous-suspension clay (25 mg/5 mL) were applied on optical-grade quartz plates, and the plates were dried under ambient atmosphere. Ion exchange was conducted in **AzI** ethanol–water (2:3) solution (100 mg/50 mL) by immersing the dried plates for 1 day at 50°C. After a thorough washing with ethanol–water mixture, films of **Az/clay** complexes on quartz plate were obtained. Formation of the composites was confirmed by XRD.

REFERENCES

[1] Whittingham, M. S. & Jacobson, A. J. (1982). *Intercalation Chemistry*, (Academic Press).

[2] Clearfield, A. (1988). *Chem. Rev.*, *88*, 125.

[3] Ramamurty, V. et al. (1991). *Photochemistry in Organized and Constrained Media* (New York: VCH Publications Inc).

[4] Ogawa, M. & Kuroda, K. (1995). *Chem. Rev.*, *95*, 399.

[5] Yariv, S. & Cross, H. (2002). *Organo-Clay Complexes and Interactions*, Marcel Dekker: New York.

[6] Seki, T. & Ichimura, K. (1991). *Macromolecules*, *23*, 31.

[7] Okahata, Y. & Shimizu, A. (1989). *Langmuir*, *5*, 954.

[8] Ahmadi, M. and Rusling, J. (1995). *Langmuir*, *11*, 94.

[9] Ogawa, M., Hama, M., and Kuroda, K. (1999). *Clay Minerals*, *34*, 213.

[10] Chuvyrov, A. N., Mukhamedjarova, G. A., Kuvatov, Z. Kh. (1995). *Mol. Cryst. Liq. Cryst.*, *265*, 3067.

[11] van der Kooij, F. M. & Lekkerkerker, H. N. W. J. (1998). *J. Phys. Chem. B*, *102*, 7829.

[12] Kawasumi, M., Hasegawa, N., Usuki, A., & Okada, A. (1999). *Appl. Clay Sci.*, *15*, 93.

[13] Kawasumi, M., Hasegawa, N., Usuki, A., & Okada, A. (1996). *Liq. Cryst.*, *21*, 769.

[14] Ujiie, S. & Iimura, K. (1992). *Macromolecules*, *25*, 3174.

[15] Bazuin, C. G. & Brandys, F. A. (1992). *Chem. Mater.*, *4*, 970.

[16] Ujiie, S. & Iimura, K. (1993). *Polymer J.*, *25*, 347.

[17] Shimomura, M., Aiba, S., Tajima, N., Inoue, N., & Okuyama, K. (1995). *Langmuir*, *11*, 969.

[18] Vaia, R. A., Teukolsky, R. K., & Giannelis, E. P. (1994). *Chem. Mater.*, *6*, 1017.